IEEE Access
Multidisciplinary | Rapid Review | Open Access Journal

Received May 18, 2020, accepted June 7, 2020, date of publication June 10, 2020, date of current version June 23, 2020.

Digital Object Identifier 10.1109/ACCESS.2020.3001206

Efficient Image Enhancement Model for Correcting Uneven Illumination Images

ZIAUR RAHMAN[1], PU YI-FEI[1], MUHAMMAD AAMIR[1,2], SAMAD WALI[2], AND YURONG GUAN[3]

[1]College of Computer Science and Technology, Sichuan University, Chengdu 610065, China
[2]School of Information and Communication Engineering, University of Electronic Science and Technology of China, Chengdu 611731, China
[3]Department of Computer, Huanggang Normal University, Huanggang 438000, China

Corresponding author: Pu Yi-Fei (puyifei@scu.edu.cn)

This work was supported in part by the National Key Research and Development Program Foundation of China under Grant 2018YFC0830300, and in part by the National Natural Science Foundation of China under Grant 61571312.

ABSTRACT Images captured under varying light conditions have deficient contrast, low brightness, latent colors, and high noise. Numerous methods have been developed for image enhancement. However, these methods are only suitable for enhancing specific type of images (e.g., over-exposed or underexposed), and also fail to restore artifact-free results for various other types of images. Therefore, to meet this goal, in this paper, we present an automatic image enhancement method, which is capable of producing quality results for all types of images captured under uneven exposure conditions (e.g., backlit, non-uniform, over-exposed, one-sided illumination and night-time images). Firstly, images are categorized using a convolutional neural network (CNN) to determine their class, and different values of weight coefficients are achieved for further processing. Then, images are converted into photonegative form to obtain an initial transmission map using a bright channel prior. Next, L1-norm regularization is adopted to refine scene transmission. Besides, environmental light is estimated based on an effective filter. Finally, the image degradation model is applied to achieve enhanced results. Furthermore, post-processing of the images is comprised of two steps, such as denoising and details enhancement. The denoised model is only applied when the images are captured in extreme low-light conditions. Whereas, a smooth layer is obtained using L1-norm regularization to enhance details in partially over-and under-exposed images. Extensive experiments reveal the effectives of the proposed approach as compared to other state-of-the-art algorithms.

INDEX TERMS Exposure correction, low-light conditions, details enhancement, image degradation model.

I. INTRODUCTION

Images captured in inadequate illumination conditions or the images obtained directly from the output of different imaging sensors descends the overall visual quality of the images. One of the common factors is the low-light imaging conditions, which will hide the visual information and the visual quality of these images is not always guaranteed. Fully revealing the visual information under dark light imaging conditions and improving the image quality of these images have practical application significance in all aspects. For humans, it is simple to process the images. However, image features with which we are specifically interested cannot be extracted by machines properly from dark images. Then, any kind of analysis or interpretation of images having dull colors and poor visibility, degrade the performance of numerous ultimate image processing tasks including object detection, segmentation, forensics, and other imaging systems. In the last decades, substantial improvements have been achieved in digital cameras, including sensitivity and resolution, to get images with perfect contrast. Even with these improvements, one cannot capture a well-exposed image without having perfect light conditions. Typically, consumer devices are not specifically intended to be weather-proof. Hence, images inevitably obtained under uneven illumination conditions can generally be divided into different typical situations, as shown in Figure. 1. Mainly, the problem that can be overlooked by previous research is that it is not necessary to change the overall image appearance pixel by pixel. It is valuable to know which parts of the image need to be retained and which

The associate editor coordinating the review of this manuscript and approving it for publication was Ehsan Asadi.

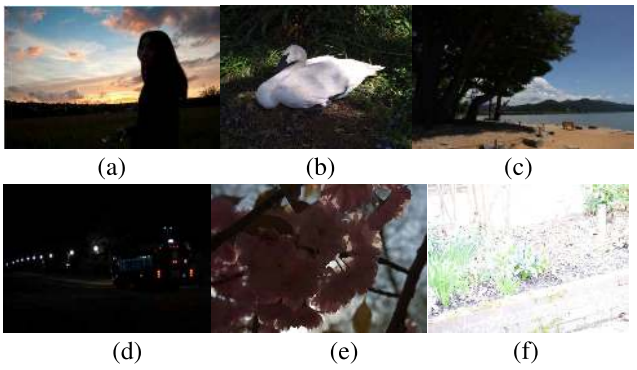

FIGURE 1. Examples of images captured under uneven illumination conditions i.e., (a) backlit (b) non-uniform (c) one-sided illumination (d) nighttime (e) normal contrast and (f) over-exposed.

parts need to be enhanced. This is ignored in most related models, which tends to produce over-enhanced results. Even, commercial software, i.e. Adobe Photoshop and Lightroom, allow users to manually retouch photos, but it is still hard for non-experts. Similarly, the use of ''Auto Tone'' in Lightroom and ''Auto Enhance'' in iPhone allow users to enhance images on a single click. But, for images having uneven illumination may fail because of keeping an automatic balance of all appearance factors such as contrast, brightness, saturation, and so on. Consequently, to precisely address these issues, the image enhancement methods widely required to work well for all types of images. Therefore, image enhancement is still a challenging task. Subsequently, it is highly subjective and non-linear. Over the years, the research community have invested a lot of efforts to address various problems of under-exposed images. Early techniques have performed histogram equalization [1], [2], or transformation functions [3]–[6]. These methods have achieved somehow good performance however, infancy in improving the overall quality of the images due to over-saturation in the uniform areas of the images.

Likewise, many subsequent methods [7]–[10] based on the famous Retinex theory (RT) [11] and defogged model [12]–[14] are also developed to achieve high performance. Mostly, it is utilized for nighttime images and used constant parameters. Other researchers used data-driven image adjustment by applying machine learning algorithms [15]–[17] or deep convolutional neural network [18]–[20]. However, these methods are still inadequate in their experimental outcomes, e.g., local overexposure, unclear details and color distortion. Moreover, these methods are limited to enhance specific types of images such as nighttime, backlit and non-uniform. Based on these research patterns and challenges above mentioned, there is still a need for a robust solution that can enhance different types of poor-quality images at the same time. Therefore, to meet this goal, in this paper, we present an automatic and unique approach for enhancing images captured in a changing light environment. The proposed method is based onto the idea that why the traditional approaches produce poor visual quality results despite their ability to avoid perceptual consistency and efficiency of enhancement for the specific types of images. Extending our discussion about the previous enhancement techniques, although numerous algorithms have performed well for particular lighting impairments, but sometimes they required tedious or manual parameters setting. For instance, the loss of important details in the enhanced version of the image is unacceptable since they may not keep edges consistency.

For this reason, we came up with a novel idea of classifying all types of degraded images and also determine their weight coefficient values for robust results. Similarly, the transmission map and environment light estimation are key factors for image degradation model (IDM). We estimated both initial and refined transmission map, which plays an important role to produce better-perceived quality in the images. Furthermore, one of the important observations of partially underexposed images is that they have uniform brightness and contrast. Accordingly, in the post-processing step, the estimated refined transmission map also utilized for partially low-light images, which helps to generate cleaned and detailed enhancement results. Furthermore, the maximum value of weight coefficient selected for enhancing the more latent contents in extreme dark images e.g., low-light or nighttime images. Therefore, more chances of color and brightness distortion while increasing visibility. We solved this issue for these images by utilizing the denoise model. Hence, our approach provides a robust and unique solution to enhance all types of images. To sum up, our approach has solved the critical problems of image enhancement and much efficient as compared to previous techniques. The traditional models have been developed to solve particular problem of low-light images as well as their models are application depended. However, the authors' model provides an ending in the sense that its empirical findings help to bring closure and illuminating the solution of major problems broadly and reflectively.

In this work, a deep convolutional neural network (CNN) is designed to classify images into different classes. The input image and enhance degree are selected based on a trained model. The main purpose of this classification task to provide images for enhancement framework along with specific enhance degree. Second, we estimated the initial transmission map using an effective bright channel prior and edge-preserving filter. Third, we refined the transmission map based on L1-norm regularization. Fourth, we introduced the idea to extract the detail layer by subtracting a piece-wise smooth layer from the original image and produce detail enhanced results from partially underexposed images. On the other hand, the denoised model is only adopted for images captured in a complex light environment. This arrangement of our proposed method enhances all type of illumination degraded images automatically.

The remaining sub-sections of this paper as follows. Section II presents the related work of state of the art low-light

image enhancement methods. The proposed method is discussed in details in section III, while section IV contains the experimental results and discussion. Finally, conclusion and future work are presented in section V.

II. RELATED WORK

Perfect light conditions are mandatory. Since, without having ideal light conditions, images always obtain in poor perceptual quality, which reduces the performance of vision systems. During the last decade, prior researchers have invested considerable efforts to enhance images captured in changing and poor light environment. In this section, we comprehensively review the existing approaches to image enhancement, which are either suitable to enhance individual or more types of poor-quality images. The histogram equalization (HE) is the most widely adopted technique, which improves image contrast by keeping the pixel intensities flat for the whole image and improve the dynamic range. It has been widely adopted in many applications to solve different problems, including object recognition and detection [21]. Subsequently, different variations of HE is also used for medical and natural images [1], [22]–[25]. However, these methods yield unnatural results by keeping distance among neighbouring pixels. Likely, another efficient way to improve the contrast of an image is the mapping of pixel intensities through sigmoid function. Most of existing methods typically use local intensity mapping because global mapping may produce distortion. Furthermore, Bennett and McMillan [4] decomposed image into two main layers, i.e. base layer and a detail layer, their method preserved the image details by applying different mapping functions on these two layers. Yuan and Sun [6] proposed an exposure correction method, which performed two operations on the input image, i.e., region segmentation and high-level feature measurement. The computed luminance-aware mapping for each region produces good results. Zhang *et al.* [26] decomposed input image into various tone-mapped versions and produced a well-exposed image by applying progressive fusion. Subsequently, they adopted local sigmoid mappings and global smooth transitions, which are difficult to enhance images with irregular exposure.

Furthermore, researchers have solved the problem of irregular exposure and various problems related to image enhancement using RT. According to RT, a low-light image is the pixel-wise representation of reflectance and illumination. Jobson *et al.* [27] made an early effort to this issue, but overall their model deficient to produce natural look in images. Whereas, other subsequent RT based algorithms along with slightly modifications notably improved the visibility of low-illumination image [9], [28]–[32], [72]. However, these methods may also effectuate visual factors such as color distortion, loss of important details, especially the images captured under non-uniform light conditions. Furthermore, Dong *et al.* [12] introduced a dehazed model, which tackles the problem for images captured under non-uniform or extreme light conditions. They inverted the input image, which looks like hazy image and produced better results by applying the dehazed model. Besides, Wu *et al.* [33] used the dehazed model specifically for nighttime images. Their obtained results look visually unpleasant, and they have not tackled the noise in extreme dark images.

Moreover, Wang *et al.* [34] developed a light scattering model to enhance low-light images. Their method estimated atmospheric light from inverted images and mean-standard-deviation that directly uses on different image patches indicated by superpixels. The model was suitable for images taken under uniform light conditions. However, it is also not efficient to handle the noise in enhanced results. Yu *et al.* [35] proposed a technique based on physical lighting. According to their model, RT based radiation reflection can be used for initial environmental light. Besides, they estimated the environmental light along with details loss constraint and attenuation rate of light-scattering via iterative adjustment. The model was used to enhance both bright and dark contents while preventing the effect of over-enhancement. However, this model is not only appropriate for non-uniform images but also yield pseudo color effect. Extending the discussion, Fu *et al.* [36], used an effective fusion-based approach to enhance the perceptual quality of degraded images. The method also adopted HE, which futile to extract features from very dark contents and produce vivid colours. Ko *et al.* [37] developed a variational framework for image enhancement, which minimizes smoothness constraint and total variation that significantly reduces the noise while boosting the brightness of dark regions. Additionally, it can also preserve the edges well. However, the method required high computational cost and limited to a specific type of low-light images. Moreover, Yang *et al.* [70] proposed a two step illumination estimation approach for low-light image enhancement. In this method other popular algorithms like Retinax, weighted variational and denoising models were also used to achieve quality results from low-light images.

While we investigate the significance of traditional approaches, researchers also widely used learning-based techniques, which are quite useful for numerous applications. Yan *et al.* [38] introduced an automatic way to adjust photos using deep learning strategy. Their method extracted bundled features along with pixel-wise descriptor based on nonlinear mapping function. This approach is suitable for images having normal or uniform contrast and also depend on both object detection and scene parsing while collecting contextual features. In the proposed work of Gharbi *et al.* [39] used deep learning that can enhance images in a real-time manner. On other hand, their architecture also explored other tasks such as dehazing, colourization and matting. Lv *et al.* [40] developed a multi-branch network to identify rich features. They used the enhancement process via different levels of network and the final enhanced results obtained using sub-nets branch fusion. The model achieved quality results and filtered noise while amplifying the brightness of backlit and non-uniform images. Chen *et al.* [41] designed generative adversarial networks (GANs), which learns the enhancement

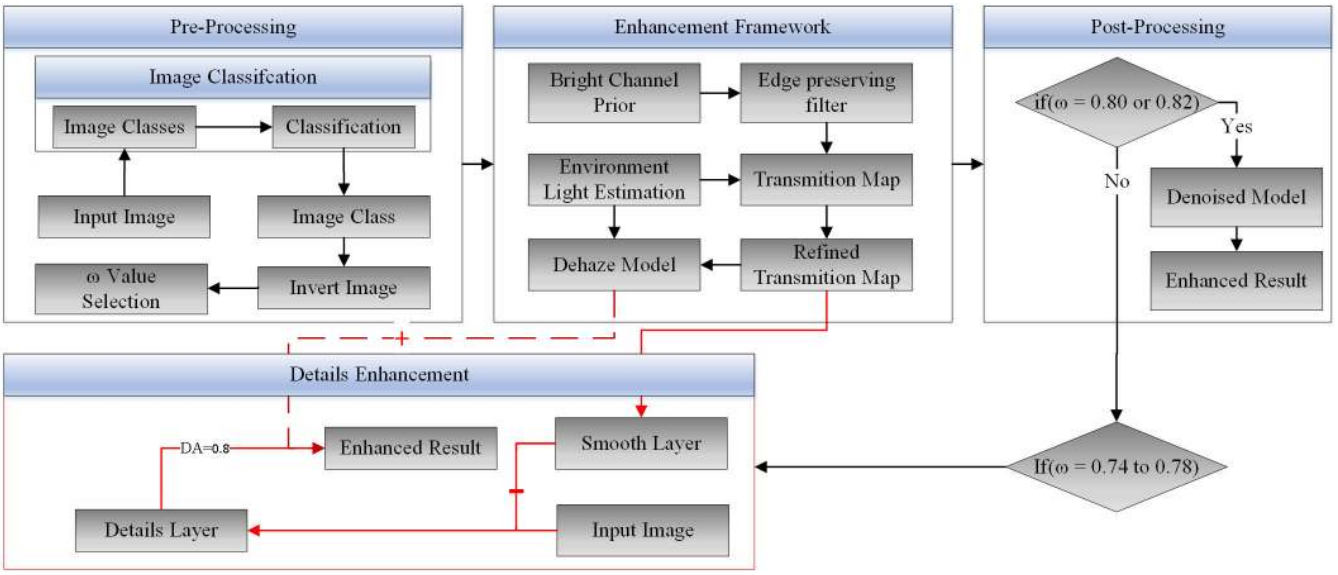

FIGURE 2. The overall flow of proposed model.

process from a given set of images. The model attained well-enhanced results, specifically from images having uniform contrast. However, the approach may fail to reduce noise from dark regions of the image. Additionally, unable to handle halo artifacts while enhancing images having a high dynamic range. Recently, Wenqi Ren *et al.* [42] addressed the visibility of low-light images via a hybrid network. The deep model adopted a content stream and edge stream to enhance visibility and edge information, respectively. However, the model unable to maintain the colour constancy. Due to the dull colours, the improved results look perceptually unnatural. Guo *et al.* [43] presented a pipeline network based on discrete wavelet transform and multi-scale retinex. The method performs well for both real-world and synthetic images, but their overall model performance is not sufficient for some particular type of images.

III. PROPOSED METHODOLOGY

We developed a hybrid model based on image degradation and deep learning models for enhancing all type of images suffered from various illumination conditions. Figure 2 describes the workflow of our proposed algorithm. The three components of our model are: (1) pre-processing (2) enhancement framework (3) post-processing. In the pre-processing step, we achieved the image classification task and converted images into photonegative form. Besides, we have assigned several values of ω to various image classes. In the enhancement framework, we developed the image degradation model. In the post-processing step, we have achieved two important tasks, i.e., image denoising and details enhancement. The denoise algorithm has applied on backlit and nighttime images when the value of enhance degree is $\omega = 0.80$) and $\omega = 0.82$. However, the details enhancement has applied on normal contrast, side-illumination, and non-uniform images when the value of enhance degree is $\omega = 0.74$), $\omega = 0.76$) and $\omega = 0.78$.

A. DEEP LEARNING-BASED IMAGE CLASSIFICATION

Over the past few decades, due to the rapid use of deep learning technology, lots of advancements have been achieved in image processing, particularly the adoption of CNN. The highest accuracy for numerous tasks (e.g., classification and recognition) have been yielded for many applications. The main reason behind these achievements is not only massive datasets from learning-based methods but also new techniques and speedy improvements in deep network architectures. In this paper, we used an existing pre-trained GoogLeNet network [44] which is trained to classify a thousand different classes of images. The selection of this pre-trained model has saved lots of computational cost and reduces the efforts for unusual parameter settings. This can be a lot easier than training a network from scratch. However, we modified the network and trained it to classify five different classes of low-light images. In this paper, the images collected for training process divided into five folders and each folder contained one hundred images. The training process resumed by replacing the last couple of layers. Following are the changes we made in the GoogLeNet model:

- The last *FullyConnectedLayer* got the number of classes that used to recognize and it is replaced with another new *FullyConnectedLayer* and set the output size to 5 because we have 5 classes.
- The *ClassificationOutputLayer* of the GoogleNet which is trained on thousand different classes is replaced with blank classification layer to learn the new classifications.
- The training parameters such as the initial learning rate is set to 0.001, the learn rate drop factor is set to 0.3,

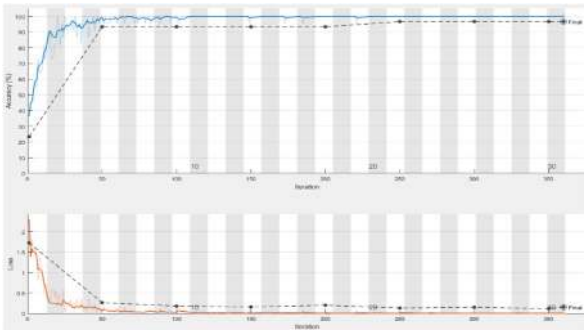

FIGURE 3. The dynamic graph of training process for accuracy and loss.

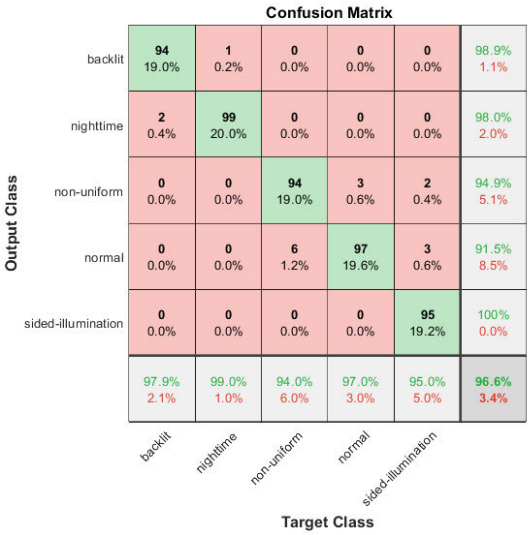

FIGURE 4. Confusion matrix for training process.

TABLE 1. Comparison of our model based on precision, recall and f-measure.

Images	Precision	Recall	F-measure	Accuracy
Training	0.9668	0.9658	0.9663	0.9658
Testing	0.9785	0.9780	0.9783	0.9780

learn rate drop period is set to 3, epochs are set to 30, maximum iterations are set o 360, and mini batch size is set to 32. These parameters setting most suitable choice for our experiments.

Furthermore, after several changes in to GooglNet, the modified pre-trained network drastically achieved the same classification task for five different classes of images. Besides, both accuracy and loss of the training process can be seen in Figure 3. Moreover, Figure 4 and Figure 5 depict the performance of the proposed method based on confusion matrix. Furthermore, the classification accuracy of the model is calculated on typically used accuracy measurement criterion, i.e., recall, precision, accuracy, and f-measure as shown in Table 1. The mathematical representation of the measurement criterion is given

FIGURE 5. Confusion matrix for testing process.

as follows:

$$precision = \frac{Tp}{TP + FP} \tag{1}$$

$$recall = \frac{FP}{FP + TN} \tag{2}$$

$$accuracy = \frac{TP + TN}{TP + TN + FP + FN} \tag{3}$$

$$f - measure = 2 * \frac{precision * recall}{precision + recall} \tag{4}$$

where FP, TN, FN and TP refer to false positive, true negative, false negative and true positive, respectively. The assessment results can be seen in Table 1.

To sum up, in this paper, various degraded images are classified to handle visual appearance via dehaze model. We integrated classification model in the pre-processing stage because no universal model exist to measure the light intensity or separate out degraded images on the basis of their visual appearance. For this, we have tested our model by providing several ω values and observed the effect of these values on different degraded images. Hence, we chosen different ω values for each classified image classes and improved the perceptual quality.

B. IMAGE DEGRADATION MODEL

The well-known IDM is widely implemented for removing haze from images. To the best of author's knowledge, the IDM has been implemented only for nighttime images as well as with constant ω values. For example, in [14], presented model is IDM, which is suitable for enhancing nighttime images and they have used constant parameter, i.e., $\omega = 0.65$. In fact, this paper discusses IDM from a number of viewpoints. Inspired by the model presented in [45], it can also be used for images which are degraded due to low-light conditions. Mathematically it can be expressed

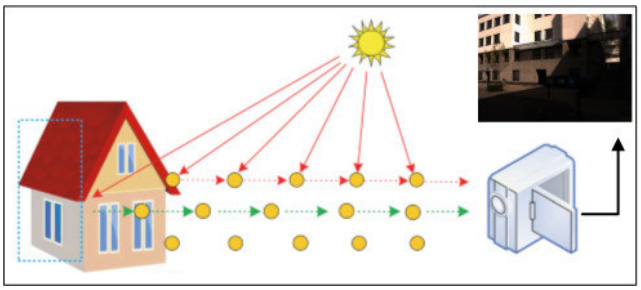

FIGURE 6. The main idea of IDM, the red solid arrows show global atmospheric light, green dotted arrows direct attenuation, red dotted arrows airlight. The light received by the camera from the scenes is attenuated along with sight and the incoming light is mixed with airlight. Thus, the perceptual quality of images is degraded.The amount of degradation based on the distances between the camera and the target scene points.

as follows:

$$\mathrm{I}_{mg}(x) = t(x)J(x) + (1 - t(x))A^c/\omega \tag{5}$$

As can be seen in (5), the model consists of three important components such as global airlight A, which is caused due to scattering of illumination in the atmosphere. The illumination may have multiple sources including diffuse skylight, direct sunlight and reflected light. $J(x)$ represents a surface radiance, while $t(x)$ is the transmission map. As shown in Figure 6, the surface radiance and airlight is the mixture of degraded pixels. Even though the IDM is same as the defog model adopted for detaching haze from images such as [46], this dehazed model could not be used directly for low-light image enhancement. Moreover, the dark channel prior (DCP) in defog model is suitable for haze-free images, but the pixel intensities are very low in low-light images. Hence, DCP model cannot be used to improve low-light images.

C. BRIGHT CHANNEL PRIOR (BCP)

Instead of DCP, we estimated $t_i(x)$ based on BCP and further refined it for enhancing low-illumination images. According to BCP, the most patches of inverted image ($I = 225 - I$) has normalized in the range i.e., [0, 1]. Moreover, by applying BCP the shadow contents of image become brighter due to inverted effect. Specifically, there should be larger value for maximum intensity in inverted image patch. The BCP can be defined as follows:

$$J^{bc}(x) = \max_{y\in\Omega(x)} \left(\max_{c\in\{r,g,b\}} (J^c(y) \right) \tag{6}$$

where $J^{bc}(x)$ is the observed bright prior, $\Omega(x)$ is local patch and J^c denotes all three channels of image. The inverted low-light image pixel values in the range of [01], thus it can be expressed as:

$$\max_{y\in\Omega(x)} \left(\max_{c\in\{r,g,b\}} (J^c(y) \right) \to 1, \min_{y\in\Omega(x)} \left(\min_{c\in\{r,g,b\}} (1 - J^c(y) \right) \to 0 \tag{7}$$

According to IDM i.e., given formula (5), both transmission map $t(x)$ and airlight A^c are needed for recovering $J(x)$. Thus, the min operation is taken on local patch of inverted image can be seen in (8), we have:

$$\max_{y\in\Omega(x)} \left(\max_{c\in\{r,g,b\}} I^c(y) \right) = t_i(x) \max_{y\in\Omega(x)} \left(\max_{c\in\{r,g,b\}} (J^c(y)) + (1 - t_i(x))A^c \right) \tag{8}$$

where $t_i(x)$ is the initial transmission map (ITM), A^c denotes values of airlight for color channels and J^c is the intensity for all image channels. Since, using formula (7), the ITM can be estimated as follows:

$$t_i(x) = \frac{\left(\max_{y\in\Omega(x)} \left(\max_{c\in\{r,g,b\}} I^c(y) \right) - A^c \right)}{1 - A^c} \tag{9}$$

The Eq(9) can also be written as follows:

$$t_i(x) = 1 - \omega * \frac{1 - \left(\max_{y\in\Omega(x)} \left(\max_{c\in\{r,g,b\}} (I^c(y)) \right)}{1 - A^c} \tag{10}$$

where $\Omega(x)$ is local patch centered at pixel x and ω denotes weight coefficient. In order to control the enhancement process different values of ω are selected for each class of images. Without applying filter, we get the transmission map same as DCP, which is utilized for dehazing process. Our task is to enhance low-illumination images. Hence, we applied the edge-aware filter [47] on BCP to slightly preserve the edges, in this way we get clean ITM different from DCP map as shown in Figure 8.

D. CONTEXTUAL REGULARIZATION (CR)

Typically, the pixels located in a local patch share same depth value. Therefore, according to this assumption, a patch-wise ITM is derived. However, this assumption may produce halo artifacts due to abrupt changes on the image edges. This issue is addressed using weighting function (WF) i.e.,

$$WF(x, y) \left(\sum_{c\in\{r,g,b\}} t^c(y) - t^c(x) \right) \approx 0 \tag{11}$$

where x and y both are neighboring pixels. When $WF(x, y)$ is equal to zero, then $t(x)$ will be cancelled. To choose an optimal $WF(x, y)$, this WF plays an important role. Furthermore, variation in depth values generally occur on edges. We can calculate the change in local color pixels and luminance based on two weighting functions as follows:

$$WF(x, y) = e^{-\left\| \left(\sum_{c\in\{r,g,b\}} I_{mg}{}^c(x) - \mathrm{I}_{mg}{}^c(y) \right) \right\|^2 / 2\sigma^2} \tag{12}$$

$$WF(x, y) = (|\log(x) - \log(y)|^{\alpha} + \varepsilon)^{-1} \tag{13}$$

where in (11), $I_{mg}(x) - I_{mg}(y)$ is the difference between color vectors, σ is prescribed parameter, while in (13), is log-based luminance of $I_{mg}(x)$, $\alpha > 0$ controls the brightness between all pixels, and ϵ value is set to 0.0001 for avoiding division by zero. Moreover, we used L1-norm with weighted constraints by taking integral of entire image domain can be expressed as:

$$\int_{x\in\Omega} \int_{y\in w_x} WF(x, y) \, |t(x) - t(y)| \, dxdy \tag{14}$$

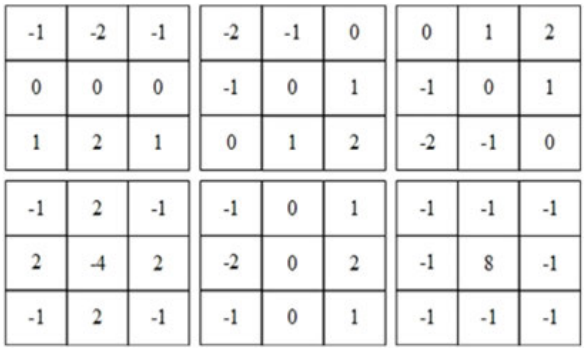

FIGURE 7. Filters bank used in this research based on Laplacian and Kirsch operators.

where Ω denotes image domain and instead of L2-norm, we adopted L1-norm because it is more robust and appropriate to outliers. Generally, the outliers occur when inaccurate contextual constraints are produced. For example, similar color adjacent pixels have disparate depth values will provide fallacious constraint as in (11).

To make easy the computation process, we further convert formula (13) in discrete form as follows:

$$\sum_{i\in I}\sum_{j\in w_i} w_{ij}\left|t_i - t_j\right| \tag{15}$$

where I and w_i indicate index set of the images pixels and w_{ij} signify the discrete form of $WF(x, y)$. The formula in (15) can be rewritten by changing order of summation and further adding the differential operators we get that, i.e.,

$$\sum_{j\in\omega}\left\|WF_j \circ (Df_j \otimes t)\right\|_1 \tag{16}$$

where ω represents index set, $\otimes$ is convolution operator, $\circ$ is operator for element-wise multiplication, and Df_j is the differentiation operator. It is also useful for using differential operators in (19). Figure 7, depicts filter bank used in our study.UY7 To utilize those filters formulae (12), (13) are used. In addition to this, the refined transmission map $t(x)$ is obtained by minimizing the subsequent objective function explained as follows:

$$\frac{\lambda}{2}\left\|t - t_i\right\|_2^2 + \sum_{j\in\omega}\left\|WF_j \circ (Df_j \otimes t)\right\|_1 \tag{17}$$

The first part of equation (17) shows data fidelity term of $t(x)$, to derived $t_i(x)$, whereas the second term represents contextual constraints. The regularization parameter λ is used to keep balance between two terms. Furthermore, equation (17) is optimized using variable splitting and construct sub-problems. Specifically, the auxiliary variables are introduced, which is represented by au_j, newly obtained equation (18) is shown below is another form of the cost function.

$$\frac{\lambda}{2}\left\|t-t_i\right\|_2^2+\sum_{j\in\omega}\left\|WF_j \circ au_j\right\|_1+\frac{\beta}{2}\left(\sum_{j\in\omega}\left\|au_j-Df_j\otimes t\right\|_2^2\right) \tag{18}$$

where β indicates a weight and as $\beta \to \infty$ the equation (18) solution will converge to equation (17). The minimization process of equation (18) for specified β value can be completed with other optimization in regard to au_j, and t. Firstly, solve each optimal value of au_j by fixing t, then compute an optimal t by fixing au_j. This process will continue until convergence is achieved. Furthermore, the closed-form solutions of sub-problems for this process can be unraveled efficiently. The first optimization process for keeping t fixed in equation (18), can be solved for au_j as follows:

$$\left\|W_j \circ au_j\right\|_1 + \frac{\beta}{2}\left\|au_j - Df_j \otimes t\right\|_2^2 \tag{19}$$

The above equation solving a set of independent one-dimensional problems of the given forms i.e.,

$$\min_x \ |w \cdot x| + \frac{\beta}{2}(x-a)^2 \tag{20}$$

where β, w and α are available then this problem can be calculated as:

$$x^* = \max(|a| - \frac{w}{\beta}, 0) \cdot S_{in}(a) \tag{21}$$

where S_{in} represents sign function. Furthermore, the second optimization process is solved using equation (18) for optimal value t by keeping fixed au_j as given below.

$$\frac{\lambda}{2}\left\|t - t_i\right\|_2^2 + \frac{\beta}{2}\left(\sum_{j\in\omega}\left\|au_j - Df_j \otimes t\right\|_2^2\right) \tag{22}$$

Thus equation (22) is quadratic and satisfies for optimal value of t as follows:

$$\frac{\lambda}{\beta}(t - t_i) + \sum_{j\in\omega} D_j^T \otimes (D_j \otimes t - u_j) = 0 \tag{23}$$

where D_j^T indicates the filter. We finally calculated the refined transmission map t_r by applying a two-dimensional fast Fourier transform on equation (23) as given below:

$$t_r = F^{-1}\left(\frac{\frac{\lambda}{\beta}F(t_i) + \sum_{j\in\omega}\overline{F(D_j)} \circ F(u_j)}{\frac{\lambda}{\beta} + \sum_{j\in\omega}\overline{F(D_j)} \circ F(D_j)}\right) \tag{24}$$

where F^{-1} is the inverse Fourier transform of $F(\cdot)$ and $\overline{(\cdot)}$ indicates complex conjugate. During the process of refined transmission map estimation, the β value iteratively increases from initial value i.e., $\beta_0 = 1$ to maximum value, i.e., $\beta_{max} = 2^6$ along with scaling factor (2.82), which alternatively compute the sub-problems mentioned in equation (19) and (20). Figure 8 describes the process of refined transmission map estimation.

E. ENVIRONMENTAL LIGHT ESTIMATION

The process of light estimation for images taken under uneven light conditions must be adjusted for different areas. In dehaze process, atmosphere illumination is global constant

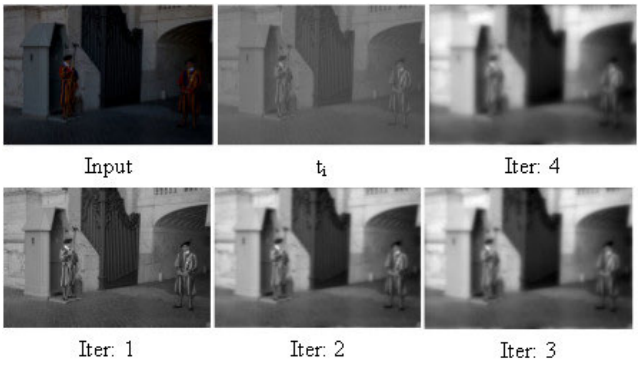

FIGURE 8. An illustration of refined transmission map estimation. This process rapidly converges after four iterations. The parameters used in this process are, input image, initial transmission t_i, $\lambda = 1.0$ and $\alpha = 0.7$.

and it is typically measured with the brightest pixels. However, it does not appropriate in dim light conditions such as dark light is not as similar as daytime light and it is not as intense as sunlight. Besides, there may be many sources of illumination in the low-light conditions, i.e., moon light and artificial light. According to [45], after applying normalization and filtering, we obtain the environmental light A^c. Furthermore, We use A^c to define and estimate the atmosphere light using an area adaptive technique. The simple but yet effective adaptive method utilized to calculate the airlight. The A^c can boost the image adaptively but it is little bit weak. Hence, we modify A^c as:

$$A^{c'} = A^c/2 \tag{25}$$

In Eq (25), $A^{c'}$ is closer to zero than A^c, which implies that the estimated environment light is closest to 0 in our model. The darker area is further improved. Moreover, we used a 7×7 filter as shown in Figure 10.

Compared to median filtering and average filtering, our filter performs well in the texture areas.

IV. EXPERIMENTAL RESULTS

This section contains extensive experiments to validate the performance of our proposed model by comparing it along with various contemporary algorithms. All experiments in this research were implemented in MATLAB 2019a and PC with the specifications of Windows 10, 3.5-GHz CPU, and 8 GB of RAM.

A. DATASETS AND QUALITY ASSESSMENT

1) BENCHMARK DATASETS

The images used for classification task or evaluation process of image enhancement based on several benchmark datasets. We made clear that the images in these datasets taken under various lighting conditions. The random selection of these images from the datasets, i.e., LIME [10], NPE [7], MF [36], MEF [48], VV[1] and FiveK [15].

2) EVALUATION METRICS

The quantitative performance of proposed model is evaluated on four commonly used metrics such as discrete entropy (DE) [49], natural image quality evaluator (NIQE) [50], visual information fidelity (VIF) [51] and visibility level descriptor (VLD) [52]. Mostly publically available benchmark datasets for image enhancement task do not supply ground-truth results. Hence, the assessment algorithms quantify the performance either in non or full-reference manner. The non-reference algorithm only needs enhanced image as an input to predict the final score, while the full-reference algorithm required both original input image and enhanced image. Typically, the high score from DE, VIF and VLD algorithms show that the overall visibility of low-illumination images is well improved. On other hand, low scores of NIQE denote the high degree of naturalness.

[1]https://sites.google.com/site/vonikakis/datasets

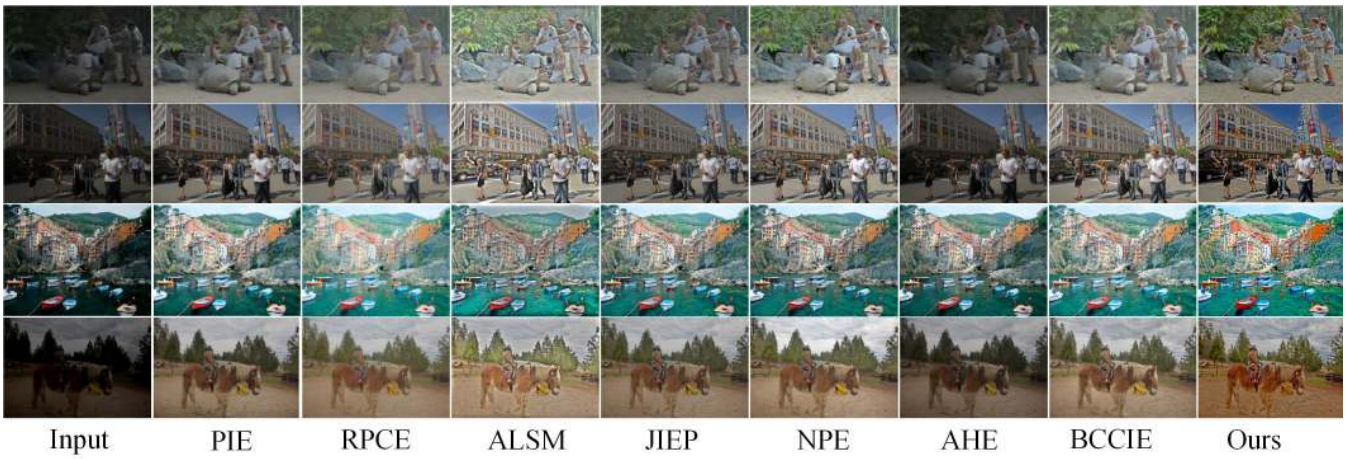

FIGURE 9. Visual results obtained from normal contrast images by proposed and compared approaches.

TABLE 2. The predicated scores between our model and other traditional algorithms.

Dataset	WVM[8]		JIEP[9]		NPE[7]		LIME[10]		DPE[41]		Ours	
	DE	NIQE	DE	NIQE	DE	NIQE	DE	NIQE	DE	NIQE	DE	NIEQ
MEF	7.13	3.77	7.43	3.51	7.16	3.59	7.43	3.68	7.08	3.76	7.56	3.37
NPE	6.84	3.83	7.34	3.51	7.33	3.47	7.43	3.11	7.13	3.62	7.64	3.02
MF	7.19	3.22	7.21	3.17	7.22	2.98	7.64	3.08	7.03	3.41	7.74	2.81
LIME	6.8	4.21	7.3	3.87	7.36	3.99	7.39	3.96	6.87	4.31	7.45	3.57
FiveK	7.37	2.95	7.51	2.76	7.6	2.65	7.65	2.89	7.46	3.17	7.81	2.68
VV	7.13	3.11	7.18	2.79	7.1	2.87	7.19	2.88	6.93	3.17	7.25	2.75

1	1	1	1	1	1	1
1	4	4	4	4	4	1
1	4	16	16	16	4	1
1	4	16	64	16	4	1
1	4	16	16	16	4	1
1	4	4	4	4	4	1
1	1	1	1	1	1	1

FIGURE 10. A representation of filter used for light estimation.

B. RESULTS AND DISCUSSION

Based on these literature insights, the algorithms have been developed for improving the visual quality of low-illumination images is limited to a specific type of images. In this paper, a novel research study has been carried out that unveils a new model for adjusting uneven illumination images. Moreover, to check the efficiency of the proposed method number of experiments have been carried out. Both manual and automatic methods are implemented to validate the performance of the proposed model. Since every user enhances the images based on personal preferences. Therefore, to achieve more diversity in the perspective of results, we have provided user interaction. Moreover, the experimental results are obtained from different image classes in a one-on-one fashion.

Firstly, the images randomly taken from five datasets and divided into five folders. Each folder contains 100 images and represents different image classes such as backlit, nighttime and so on. Based on manual procedure, the users can interact and choose different values of details amplification (DA), i.e. $0 < DA < 1$ and weight coefficient ω, i.e., $0 < \omega < 1$ for image classes. However, we manually initialized several ω values for each image class i.e., for slightly contrast degraded images $\omega = 0.74$, non-uniform $\omega = 0.76$, one-sided illumination $\omega = 0.78$, backlit $\omega = 0.80$, and nighttime $\omega = 0.82$. Furthermore, the post-processing step is utilized for all type of images as shown in Figure 2. Besides, the details enhancement process is performed when a particular image class is equal to values. However, the denoising model is applied on backlit and extreme low-light images. The quantitative results of our model and comparison along with traditional approaches can be seen in Table 2. The WVM [8], LIME [10], DPE [41] and JIEP [9] achieved better visual results for low-light images, while NPE [78] is suitable for non-uniform images. However, these methods unable to reveal dark contents from backlit and extreme low-light images. According to the specified parameters and predicated results made sure that our model achieved better performance in terms of DE and NIQE.

TABLE 3. Average scores of quantitative metrics estimated for enhancing slightly contrast degraded images.

Methods	DE	NIQE	VIF	VLD
BCCIE [25]	7.33	18	1.52	1.54
NPE [7]	7.34	17.23	2.49	2.32
JIEP [9]	7.36	17.49	1.89	1.85
RPCE [31]	7.29	17.77	1.17	1.88
ALSM [34]	7.4	17.09	3.32	2.37
PIE [30]	7.28	18.58	2.26	1.92
AHE [24]	7.33	17.56	1.1	1.16
Ours	7.59	16.21	3.73	2.93

Extending the validation process, since amplifying specific amount of contrast or brightness is required while enhancing uneven illumination degraded images. Therefore, various ω values are chosen to control the enhancement process and reveal more hidden contents. To automate the enhancement process, classification task of several image classes is achieved based on deep learning. The input images belong to which category is identified based on the classified model and different weight coefficient ω values are assigned to each image classes. We obtained the enhanced results of each image class and compared with other techniques. Firstly, we show experimental results that is produced from slightly contrast degraded images. The visual and quantitative comparison can be seen in Figure 9 and Table 3, respectively. It is revealed from visual results that classical methods enhance the dark contents but still their results have hazy effect. Moreover, the results produced by ALSM [34] suffer from the over-saturation artifacts. However, BCCIE [25], NPE [7] and RPCE [31] enhanced more hidden contents as compared

FIGURE 11. Visual results obtained from non-uniform images by proposed and compared approaches.

FIGURE 12. Visual results obtained from one-sided illumination images by proposed and compared approaches.

to JIEP [9], PIE [30] and AHE [24]. However, in comparison to other competing methods, the authors' model extract more details, enhance color, and eliminate hazy effect.It can be clearly observed from Figure 9, our model enhances all the appearance factors very well such as trees color, building texture, sky color, and visible the clouds.

Secondly, we tested the performance of the proposed model by providing non-uniform images. The images capture under non-uniform light conditions have a different visual appearance. The light intensities are not uniform in such types of images. The visual results in Figure 11 and quantitative accuracies in Table 4 show that the proposed method outperformed other algorithms in terms of perceptual quality and quantitative analysis. As shown in Figure 11, NPE [7], PIE [30], MCRN [53] and LSYIE [54] preserved the naturalness and enhanced more contents in images as compared to CVC [22], FCCE [55], and VFM [56]. Moreover, it can be clearly observed that the proposed model not only preserved the naturalness and eliminate the hazy effect, but also obtained well-saturated results.

TABLE 4. Average scores of quantitative metrics estimated for enhancing non-uniform images.

Methods	DE	NIQE	VIF	VLD
NPE [7]	7.48	16.98	2.5	2.02
PIE [30]	7.38	17.25	2.2	1.57
MCRN [53]	7.4	18.28	1.4	1.73
LSYIE [54]	7.23	18.32	1.35	1.42
FCCE [55]	7.11	18.52	1.3	1.06
CVC [22]	7.32	18.27	1.3	1.46
VFM [56]	7.02	19.83	1.26	1.38
Ours	7.58	16.85	2.87	3.01

Thirdly, the experimental results obtained using images, where a one-half portion of the entire image is dark or bright, we called them one-sided illumination degraded images. Figure 12 shows the qualitative performance, and Table 5

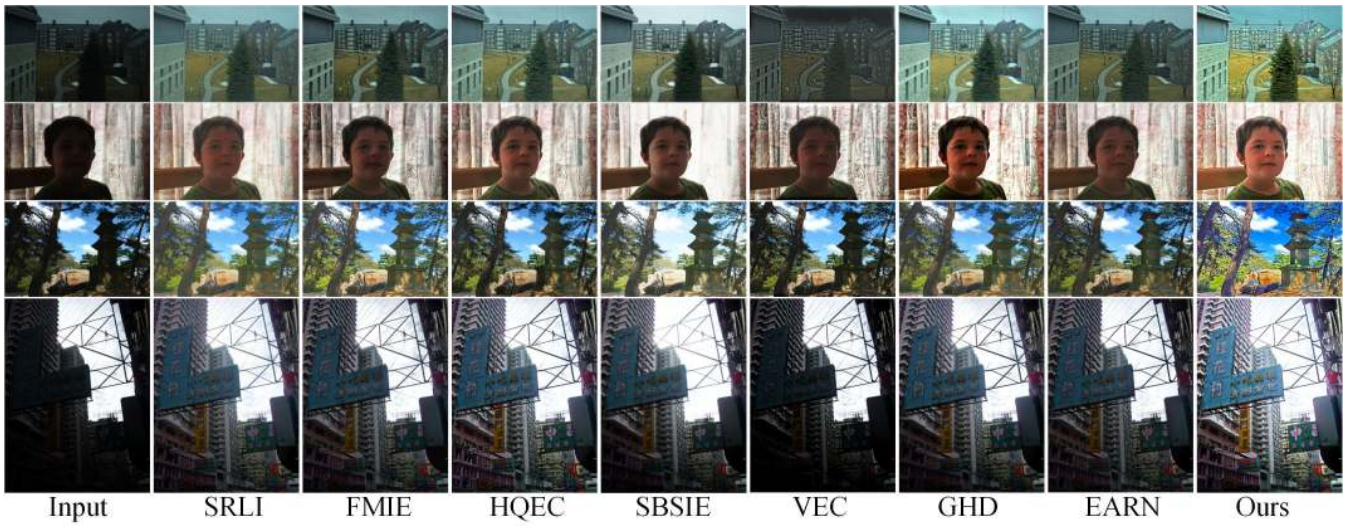

FIGURE 13. Visual results obtained from backlit images by proposed and compared approaches.

TABLE 5. Average scores of quantitative metrics estimated for enhancing one-sided illumination.

Methods	DE	NIQE	VIF	VLD
FBE [36]	7.49	17.7	1.31	2.19
APNN [43]	7.29	18.81	1.98	1.74
LIIE [35]	7.46	18.03	1.3	2.34
NIE [57]	7.33	18.39	1.29	2.18
HMCE [58]	7.58	17.45	1.48	2.18
ICCE [59]	7.15	18.7	1.98	1.51
RIES [32]	7.18	17.27	1.57	2.27
Ours	7.7	16.49	2.55	3.26

TABLE 6. Average scores of quantitative metrics estimated for enhancing backlit image.

Methods	DE	NIQE	VIF	VLD
SBSIE [62]	7.51	18.1	1.51	2.9
GHD [61]	7.34	18.26	1.81	2.61
EARN [63]	7.13	18.98	1.42	1.87
SRLI [64]	7.36	18.06	1.11	3.09
HQEC [60]	7.54	17.51	1.91	3.8
FMIE [65]	7.38	18.01	1.43	2.85
VEC [66]	6.78	18.59	1.35	2.02
Ours	7.52	16.44	1.8	3.2

TABLE 7. Average scores of quantitative metrics estimated for nighttime image.

Methods	DE	NIQE	VIF	VLD
FBE [36]	17.17	18.57	2.62	5.31
LIEMD [67]	17.21	20.21	1.16	5.05
LECARM [29]	16.85	18.68	2.65	4.19
STAR [68]	17.23	19.43	2.38	3.47
VFLIE[37]	17.01	19.14	2.84	4.42
MRIE [28]	16.99	19.87	1.39	2.14
MBLLEN [40]	17.14	17.79	5.38	6.56
Ours	17.31	17.09	6.04	8.16

presents the quantitative scores of our model and its comparison with other state-of-the-art approaches. Furthermore, it has become apparent from the Figure 12, the methods such as LIIE [35], NIE [57], APNN [43], RIES [32] and FBE [36] enhanced more contents as compared to HMCE [58] and ICCE [59]. However, they not only unable to achieve the naturalness, but their improved results look hazy and lack of saturation color. Besides, it is self-evident from the Figure 12, the proposed model produces natural feel in images and eliminates the slightly available hazy effect from images. Nevertheless, overall results confirm that the proposed algorithm outperforms other well-know techniques in terms of various appearance factors.

Fourthly, the visual appearance of backlit images looks different from other classes of images. The images taken under illumination, where the front objects look very dark but behind the objects the background of entire image with regular contrast. To amplify the contrast or brightness, both enhancement and denoising are used to achieve better visual quality. Besides, both visual and quantitative results can be seen in Figure 13 and Table 6, respectively. It is cleared from Figure 13, our model efficiently handled the visual factors such as contrast, brightness, color and detached the slightly available hazy effect in images. However, it is cleared in Table 6, the average accuracies of HQEC [60] is better in terms of VIF, VLD and DE. Besides, GHD [61] also achieved a high score in terms of VIF. Due to the misclassification of backlit images, except for NIQE, the proposed model yields second-ranked accuracies in term of DE, VLD and VIF.

Finally, to preserve bright regions and reveal more hidden contents in dark images, the proposed model enhanced dark images and also suppress noise that is occurred by amplifying brightness of entire image. Both visual and quantitative results can be seen in Figure 14 and Table 7.

The proposed model is also very helpful for correcting overexposed images. The non-linear mapping [69] i.e., $O_e(x, y) = E_n(x, y)/(1+(1-1/\max(E_n(x, y))*E_n(x, y))$

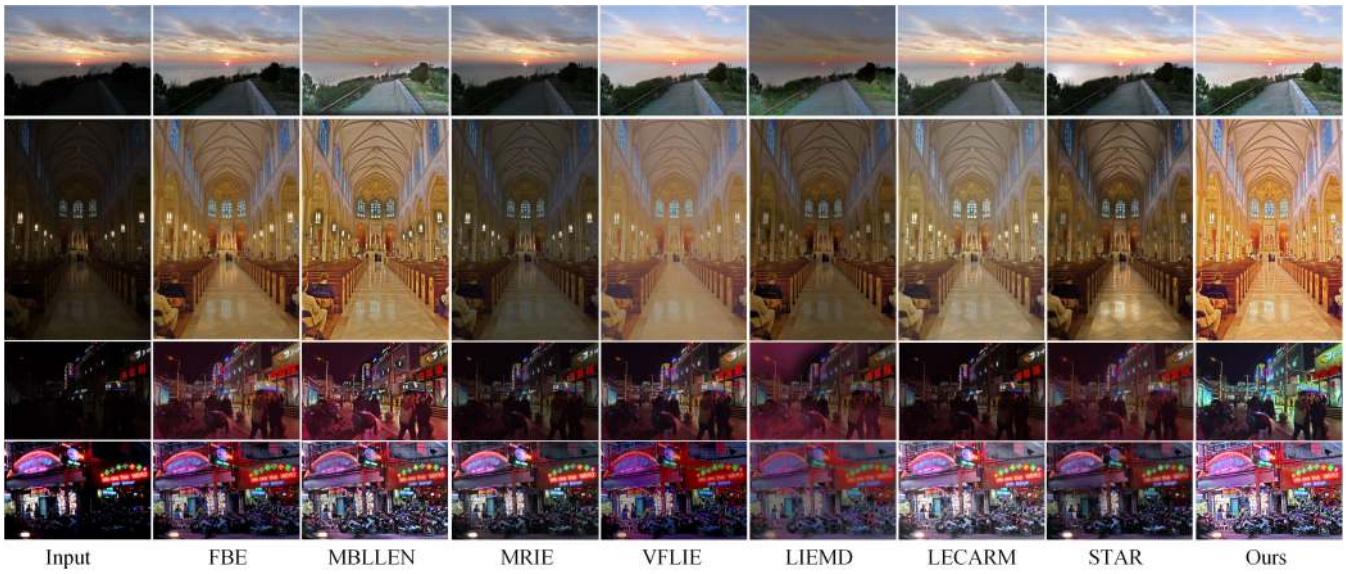

FIGURE 14. Visual results obtained from nighttime images by proposed and compared approaches.

FIGURE 15. Our model corrected the high intensities regions (a) input image (b) output achieved from post-processing step (c) output from non-linear mapping (d) combined result of (a) and (b).

FIGURE 16. Failure case of handling black regions. (a) input image (b) JIEP [9] (c) DPE [41], and (d) Ours.

is adopted to overcome this issue. Where O_n is the output of corrected overexposed image and E_n is the enhanced image, which is obtained from the post-processing step. Then, corrected overexposed results achieved by combining O_n and E_n. The Figure 15. summaries that the combined output not only compress high intensities, but also obtained well-saturated results. To sum up, our model outperformed the existing techniques in terms of overall quantitative accuracy and perceived quality in the images. This verified that our model produced well-enhanced images with adequate contrast, proper colors and natural brightness. Furthermore, no obvious flaws were noticed on overall results. Besides, our model has limitations.

Figure 16 describes that our algorithm and compared approaches are failed to produce desired results from very dark regions. It is hard to distill features of objects having extreme dark regions.

C. USER STUDY

The model presented in this paper performs two different operations to enhance images, i.e., automatic and manual. We have mentioned that automated task is performed along with a classified model. The results automatically generated by the model is hard to measure via quantitative assessment algorithms. Therefore, we performed a user study to validate the efficiency of our model by involving human expertise. For this, we generated results from proposed and several other algorithms. Specifically, to avoid subjective favoritism,

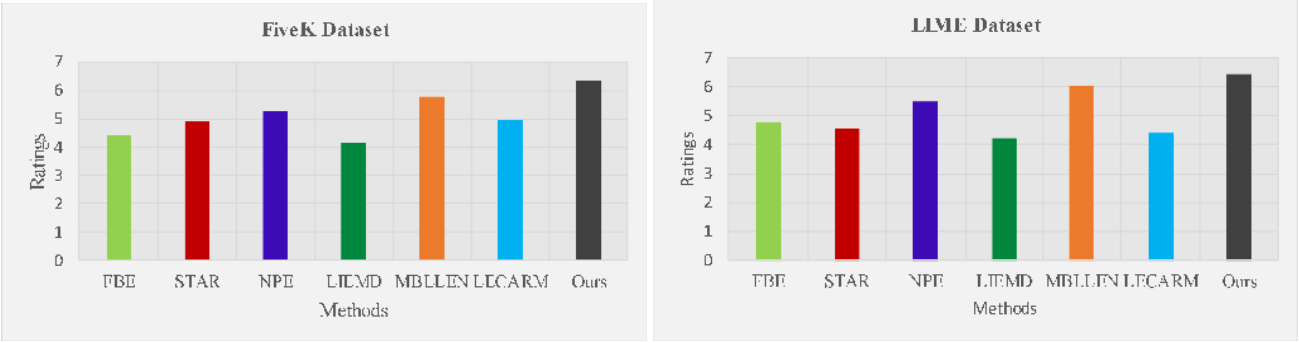

(a) (b)

FIGURE 17. A user study on generated results from two well-known datasets, i.e., (a) FiveK, and (b) LIME.

the enhanced results are grouped into several folders in random order. Total seven photographer and photo retouching experts are assigned to rate the results according to the specified requirements, i.e., (1) natural and realistic color, (2) apparent contrast and distinct details, (3) no overexposure and loss of details, (4) no color distortion. The rating score in the range from 1 to 7. The lower scores show that enhanced results have not achieved good quality while the higher scores show the best quality. After subjective analysis, all the rantings are collected and average them to get the final ranting statistics. Figure 17 demonstrates the average ratings calculated from proposed and several other models. According to the expert analysis, the generated results of our model are well enhanced. The results generated by MBLLEN [40], is a learning-based model, which is quite closer to our model performance. Their model is specifically more suitable for low-light or non-uniform images. However, the model unable to achieved good results for other types of images such as backlit and side illumination. Furthermore, the results of NPE [7] also achieved higher ratings. As the model is designed explicitly for non-uniform degraded images, therefore, this model attained lower ratings for other types of images.

D. ADDITIONAL RESULTS

The visual appearance of an image is totally different without having perfect lighting conditions. Therefore, it is very difficult to enhance the contents of various weakly illumination degraded images. However, our model provides robust solution. We randomly selected different images and observed the performance of the proposed model. The visual results are given in Figure 18. It shows, our model has revealed not only dark contents of heavily under-exposed images but also achieved visual pleasing results for other low-light images. In Figure 18, the first and third row from left to right, the images are captured in extreme light conditions. However, the images are different in visual appearance. Our model enhances the dark contents and preserve the structure of the images. The images having non-uniform illumination are presented in second and fourth row. The structure

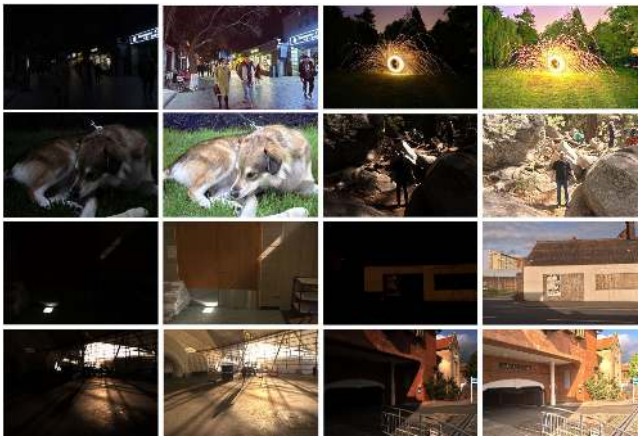

FIGURE 18. Visual results of heavily underexposed images.

FIGURE 19. The visual results of images with fine structure, the proposed model enhance and preserve the structure of the images.

and color of these images are well-preserved by our model. Furthermore, we also tested various images having fine structure (see Figure 19). The texture is preserved well by the L1-regularization used in this paper. Thus, our approach still yields reasonably successful results under the low light

conditions, where at the outset visible scene information was affected by insufficient lighting. To sum up, our model is distinct and diverse as compared to the previous approaches in a variety of perspectives. However, the traditional models have solved specific problems in image enhancement, such as highlighting and visible dim contents in limited illumination degraded images. Unlike previous approaches, we debunk the cause of why they appear to yield visually undesirable outcomes. Hence, suggested a paradigm to elucidate how to preserve perceptual consistency in particular. Therefore, we develop a dehaze model to enhance underexposed images while eliminating typical visual artifacts. Besides, in the author's view, we have offered a reliable solution for a wide variety of image enhancement applications. To ensure the effectiveness of our model, we have performed extensive experiments upon numerous datasets with the implementation of the most advanced methodologies to verify the superiority of our model.

V. CONCLUSION AND FUTURE WORK

The research findings of traditional approaches and their comparison, which is highlighted in this paper. It has been noticed that the existing algorithms either enhance the specific types of images or provide fewer analytical results. However, we introduced image enhancement model that efficiently enhance uneven illumination degraded images. The working mechanism of the proposed model is divided into three parts i.e., pre-processing, enhancement framework and post-processing. (Step 1): Image classification is performed in the first step, which effectively categorized the images into different classes. (Step 2): Similarly, the enhancement process based on IDM took place in the second part. The inverted input image along with enhance degree coefficient is provided to enhancement framework. Firstly, it estimated the initial transmission map based on the BCP and airlight along with an effective filter. Secondly, L1-norm based regularization is implemented to estimate the refined transmission map. Thirdly, the IDM is applied, and images are converted back to photonegative form as the enhanced results. (Step 3): Furthermore, the third step took place, which either performs denoising process or details enhancement. We applied the denoise model on images captured in extreme light conditions and utilized L1-norm regularization to extract more details from partly degraded images. Besides, we validated the performance of our model on six datasets. Images are randomly selected and divided into five different classes. Then, the image categorization task is achieved based on a pre-trained network, i.e., GoogleNet. The performance of image classification is evaluated in terms of well-known quality assessment criterions such as accuracy, precision, recall, and f-measure. The proposed model is also compared with various state-of-the-art approaches based on well-known quality assessment metrics such as DE, VLD, VIF, and NIQE. The experimental results show that the proposed method is superior in enhancing visual quality under uneven lighting environments. However, the empirical contributions of this research are as follows:

- It can be preferred as a better user interactive tool for photo editing applications.
- It can be helpful for the photographer to substitute a built-in component for low-light imaging devices.
- It can also be replaced as a smart intelligent component for vision systems.

Besides, in the future, this research could be further extended for adopting methods in photographic semantic analysis and image synthesis. This concept can also be extended to properly handle extremely dark regions and eliminate noise. Furthermore, we will also tackle imaging problems that may encounter due to several common weather conditions such as rain, fog, snow, and thunder. How to meet the applicability of the actual system and how to adaptively select parameters for targeted solution of different weather conditions.

REFERENCES

[1] T. Kim and J. Paik, "Adaptive contrast enhancement using gain-controllable clipped histogram equalization," *IEEE Trans. Consum. Electron.*, vol. 54, no. 4, pp. 1803–1810, Nov. 2008, doi: 10.1109/TCE.2008.4711238.

[2] C. Ooi and N. Mat Isa, "Adaptive contrast enhancement methods with brightness preserving," *IEEE Trans. Consum. Electron.*, vol. 56, no. 4, pp. 2543–2551, Nov. 2010, doi: 10.1109/TCE.2010.5681139.

[3] F. Drago, K. Myszkowski, T. Annen, and N. Chiba, "Adaptive logarithmic mapping for displaying high contrast scenes," *Comput. Graph. Forum*, vol. 22, no. 3, pp. 419–426, Sep. 2003, doi: 10.1111/1467-8659.00689.

[4] E. P. Bennett and L. Mcmillan, "Video enhancement using per-pixel virtual exposures," *ACM Trans. Graph.*, vol. 24, no. 3, pp. 845–852, Jul. 2005, doi: 10.1145/1073204.1073272.

[5] Q. Shan, J. Jia, and M. S. Brown, "Globally optimized linear windowed tone mapping," *IEEE Trans. Vis. Comput. Graph.*, vol. 16, no. 4, pp. 663–675, Jul./Aug. 2010.

[6] L. Yuan and J. Sun, "Automatic exposure correction of consumer photographs," in *Proc. Eur. Conf. Comput. Vis.* Berlin, Germany: Springer, 2012, pp. 771–785.

[7] S. Wang, J. Zheng, H. M. Hu, and B. Li, "Naturalness preserved enhancement algorithm for non-uniform illumination images," *IEEE Trans. Image Process.*, vol. 22, no. 9, pp. 3538–3548, Sep. 2013.

[8] X. Fu, D. Zeng, Y. Huang, X.-P. Zhang, and X. Ding, "A weighted variational model for simultaneous reflectance and illumination estimation," in *Proc. IEEE Conf. Comput. Vis. Pattern Recognit.*, Jun. 2016, pp. 2782–2790.

[9] B. Cai, X. Xu, K. Guo, K. Jia, B. Hu, and D. Tao, "A joint intrinsic-extrinsic prior model for retinex," in *Proc. IEEE Int. Conf. Comput. Vis. (ICCV)*, Oct. 2017, pp. 4000–4009, doi: 10.1109/ICCV.2017.431.

[10] X. Guo, Y. Li, and H. Ling, "LIME: Low-light image enhancement via illumination map estimation," *IEEE Trans. Image Process.*, vol. 26, no. 2, pp. 982–993, Feb. 2017.

[11] E. H. Land, "The retinex theory of color vision," *Sci. Amer.*, vol. 237, no. 6, pp. 108–129, 1997.

[12] X. Dong, G. Wang, Y. Pang, W. Li, J. Wen, W. Meng, and Y. Lu, "Fast efficient algorithm for enhancement of low lighting video," in *Proc. IEEE Int. Conf. Multimedia Expo*, Jul. 2011, pp. 1–6, doi: 10.1109/ICME.2011.6012107.

[13] L. Li, R. Wang, W. Wang, and W. Gao, "A low-light image enhancement method for both denoising and contrast enlarging," in *Proc. IEEE Int. Conf. Image Process. (ICIP)*, Sep. 2015, pp. 3730–3734.

[14] Z. Shi, M. Zhu, B. Guo, and M. Zhao, "A photographic negative imaging inspired method for low illumination night-time image enhancement," *Multimedia Tools Appl.*, vol. 76, no. 13, pp. 15027–15048, Jul. 2017, doi: 10.1007/s11042-017-4453-z.

[15] V. Bychkovsky, S. Paris, E. Chan, and F. Durand, "Learning photographic global tonal adjustment with a database of input/output image pairs," in *Proc. CVPR*, Jun. 2011, pp. 97–104, doi: 10.1109/CVPR.2011.5995413.
[16] S. J. Hwang, A. Kapoor, and S. B. Kang, "Context-based automatic local image enhancement," in *Proc. Eur. Conf. Comput. Vis.* Berlin, Germany: Springer, Oct. 2012, pp. 569–582.
[17] J. Yan, S. Lin, S. B. Kang, and X. Tang, "A Learning-to-Rank approach for image color enhancement," in *Proc. IEEE Conf. Comput. Vis. Pattern Recognit.*, Jun. 2014, pp. 2987–2994, doi: 10.1109/CVPR.2014.382.
[18] Y. Hu, H. He, C. Xu, B. Wang, and S. Lin, "Exposure: A white-box photo post-processing framework," *ACM Trans. Graph.*, vol. 37, no. 2, pp. 1–7, May 2018, doi: 10.1145/3181974.
[19] C. Chen, Q. Chen, J. Xu, and V. Koltun, "Learning to see in the dark," in *Proc. IEEE/CVF Conf. Comput. Vis. Pattern Recognit.*, Jun. 2018, pp. 3291–3300, doi: 10.1109/CVPR.2018.00347.
[20] C. Li, J. Guo, F. Porikli, and Y. Pang, "LightenNet: A convolutional neural network for weakly illuminated image enhancement," *Pattern Recognit. Lett.*, vol. 104, pp. 15–22, Mar. 2018, doi: 10.1016/j.patrec.2018.01.010.
[21] H. Sellahewa and S. A. Jassim, "Image-Quality-Based adaptive face recognition," *IEEE Trans. Instrum. Meas.*, vol. 59, no. 4, pp. 805–813, Apr. 2010, doi: 10.1109/TIM.2009.2037989.
[22] T. Celik and T. Tjahjadi, "Contextual and variational contrast enhancement," *IEEE Trans. Image Process.*, vol. 20, no. 12, pp. 3431–3441, Dec. 2011, doi: 10.1109/TIP.2011.2157513.
[23] C. Lee, C. Lee, and C.-S. Kim, "Contrast enhancement based on layered difference representation of 2D histograms," *IEEE Trans. Image Process.*, vol. 22, no. 12, pp. 5372–5384, Dec. 2013, doi: 10.1109/TIP.2013.2284059.
[24] C. K. Sirajuddeen, S. Kansal, and R. K. Tripathi, "Adaptive histogram equalization based on modified probability density function and expected value of image intensity," *Signal, Image Video Process.*, vol. 14, no. 1, pp. 9–17, Feb. 2020, doi: 10.1007/s11760-019-01516-2.
[25] B. Xiao, H. Tang, Y. Jiang, W. Li, and G. Wang, "Brightness and contrast controllable image enhancement based on histogram specification," *Neurocomputing*, vol. 275, pp. 2798–2809, Jan. 2018, doi: 10.1016/j.neucom.2017.11.057.
[26] Q. Zhang, Y. Nie, L. Zhang, and C. Xiao, "Underexposed video enhancement via perception-driven progressive fusion," *IEEE Trans. Vis. Comput. Graphics*, vol. 22, no. 6, pp. 1773–1785, Jun. 2016, doi: 10.1109/TVCG.2015.2461157.
[27] D. J. Jobson, Z. Rahman, and G. A. Woodell, "A multiscale retinex for bridging the gap between color images and the human observation of scenes," *IEEE Trans. Image Process.*, vol. 6, no. 7, pp. 965–976, Jul. 1997, doi: 10.1109/83.597272.
[28] H. Lin and Z. Shi, "Multi-scale retinex improvement for nighttime image enhancement," *Optik*, vol. 125, no. 24, pp. 7143–7148, Dec. 2014, doi: 10.1016/j.ijleo.2014.07.118.
[29] Y. Ren, Z. Ying, T. H. Li, and G. Li, "LECARM: Low-light image enhancement using the camera response model," *IEEE Trans. Circuits Syst. Video Technol.*, vol. 29, no. 4, pp. 968–981, Apr. 2019, doi: 10.1109/TCSVT.2018.2828141.
[30] X. Fu, Y. Liao, D. Zeng, Y. Huang, X.-P. Zhang, and X. Ding, "A probabilistic method for image enhancement with simultaneous illumination and reflectance estimation," *IEEE Trans. Image Process.*, vol. 24, no. 12, pp. 4965–4977, Dec. 2015, doi: 10.1109/TIP.2015.2474701.
[31] Q. Fu, C. Jung, and K. Xu, "Retinex-based perceptual contrast enhancement in images using luminance adaptation," *IEEE Access*, vol. 6, pp. 61277–61286, 2018.
[32] C.-C. Chien, Y. Kinoshita, S. Shiota, and H. Kiya, "A retinex-based image enhancement scheme with noise aware shadow-up function," *Proc. SPIE*, vol. 11049, Mar. 2019, Art. no. 110492K, doi: 10.1117/12.2521585.
[33] Y. Wu, W. Song, J. Zheng, and F. Liu, "A new low light image enhancement based on the image degradation model," in *Proc. 14th IEEE Int. Conf. Signal Process. (ICSP)*, Aug. 2018, pp. 379–383.
[34] Y. F. Wang, H. M. Liu, and Z. W. Fu, "Low-light image enhancement via the absorption light scattering model," *IEEE Trans. Image Process.*, vol. 28, no. 11, pp. 5679–5690, Nov. 2019.
[35] S. Y. Yu and H. Zhu, "Low-illumination image enhancement algorithm based on a physical lighting model," *IEEE Trans. Circuits Syst. Video Technol.*, vol. 29, no. 1, pp. 28–37, Jan. 2019.
[36] X. Fu, D. Zeng, Y. Huang, Y. Liao, X. Ding, and J. Paisley, "A fusion-based enhancing method for weakly illuminated images," *Signal Process.*, vol. 129, pp. 82–96, Dec. 2016, doi: 10.1016/j.sigpro.2016.05.031.
[37] S. Ko, S. Yu, S. Park, B. Moon, W. Kang, and J. Paik, "Variational framework for low-light image enhancement using optimal transmission map and combined $\ell 1$ and $\ell 2$-minimization," *Signal Process., Image Commun.*, vol. 58, pp. 99–110, Oct. 2017, doi: 10.1016/j.image.2017.06.016.
[38] Z. Yan, H. Zhang, B. Wang, S. Paris, and Y. Yu, "Automatic photo adjustment using deep neural networks," *ACM Trans. Graph.*, vol. 35, no. 2, pp. 1–15, May 2016, doi: 10.1145/2790296.
[39] M. Gharbi, J. Chen, J. T. Barron, S. W. Hasinoff, and F. Durand, "Deep bilateral learning for real-time image enhancement," *ACM Trans. Graph.*, vol. 36, no. 4, pp. 1–12, Jul. 2017, doi: 10.1145/3072959.3073592.
[40] F. Lv, F. Lu, J. Wu, and C. Lim, "MBLLEN: Low-light image/video enhancement using CNNs," in *Proc. Brit. Mach. Vis. Conf.*, 2018, p. 220.
[41] Y.-S. Chen, Y.-C. Wang, M.-H. Kao, and Y.-Y. Chuang, "Deep photo enhancer: Unpaired learning for image enhancement from photographs with GANs," in *Proc. IEEE/CVF Conf. Comput. Vis. Pattern Recognit.*, Jun. 2018, pp. 6306–6314, doi: 10.1109/CVPR.2018.00660.
[42] W. Ren, S. Liu, L. Ma, Q. Xu, X. Xu, X. Cao, J. Du, and M.-H. Yang, "Low-light image enhancement via a deep hybrid network," *IEEE Trans. Image Process.*, vol. 28, no. 9, pp. 4364–4375, Sep. 2019, doi: 10.1109/TIP.2019.2910412.
[43] Y. Guo, X. Ke, J. Ma, and J. Zhang, "A pipeline neural network for low-light image enhancement," *IEEE Access*, vol. 7, pp. 13737–13744, 2019, doi: 10.1109/ACCESS.2019.2891957.
[44] C. Szegedy, W. Liu, Y. Jia, P. Sermanet, S. Reed, D. Anguelov, D. Erhan, V. Vanhoucke, and A. Rabinovich, "Going deeper with convolutions," in *Proc. IEEE Conf. Comput. Vis. Pattern Recognit.*, Jun. 2015, pp. 1–9, doi: 10.1109/CVPR.2015.7298594.
[45] H. Koschmieder, "Theorie der horizontalen Sichtweite," in *Beitrage zur Physik der Freien Atmosphare* (Meteorol. Z), vol. 12. 1924, pp. 33–53.
[46] Z. Tufail, K. Khurshid, A. Salman, I. Fareed Nizami, K. Khurshid, and B. Jeon, "Improved dark channel prior for image defogging using RGB and YCbCr color space," *IEEE Access*, vol. 6, pp. 32576–32587, 2018, doi: 10.1109/ACCESS.2018.2843261.
[47] E. S. L. Gastal and M. M. Oliveira, "Domain transform for edge-aware image and video processing," *ACM Trans. Graph.*, vol. 30, no. 4, p. 1, Jul. 2011, doi: 10.1145/2010324.1964964.
[48] K. Ma, K. Zeng, and Z. Wang, "Perceptual quality assessment for multi-exposure image fusion," *IEEE Trans. Image Process.*, vol. 24, no. 11, pp. 3345–3356, Nov. 2015, doi: 10.1109/TIP.2015.2442920.
[49] Z. Ye, H. Mohamadian, and Y. Ye, "Discrete entropy and relative entropy study on nonlinear clustering of underwater and arial images," in *Proc. IEEE Int. Conf. Control Appl.*, Oct. 2007, pp. 313–318, doi: 10.1109/CCA.2007.4389249.
[50] A. Mittal, R. Soundararajan, and A. C. Bovik, "Making a 'completely blind' image quality analyzer," *IEEE Signal Process. Lett.*, vol. 20, no. 3, pp. 209–212, Mar. 2013, doi: 10.1109/LSP.2012.2227726.
[51] H. R. Sheikh and A. C. Bovik, "Image information and visual quality," *IEEE Trans. Image Process.*, vol. 15, no. 2, pp. 430–444, Feb. 2006, doi: 10.1109/TIP.2005.859378.
[52] N. Hautière, J.-P. Tarel, D. Aubert, and É. Dumont, "Blind contrast enhancement assessment by gradient ratioing at visible edges," *Image Anal. Stereol.*, vol. 27, no. 2, p. 87, May 2011, doi: 10.5566/ias.v27.p87-95.
[53] J. Liu and C. Jung, "Multiple connected residual network for image enhancement on smartphones," in *Proc. Eur. Conf. Comput. Vis. (ECCV)*, 2018, pp. 182–196.
[54] K. Zhan, J. Shi, J. Teng, Q. Li, M. Wang, and F. Lu, "Linking synaptic computation for image enhancement," *Neurocomputing*, vol. 238, pp. 1–12, May 2017, doi: 10.1016/j.neucom.2017.01.031.
[55] A. S. Parihar, O. P. Verma, and C. Khanna, "Fuzzy-contextual contrast enhancement," *IEEE Trans. Image Process.*, vol. 26, no. 4, pp. 1810–1819, Apr. 2017.
[56] Q. C. Tian and L. D. Cohen, "A variational-based fusion model for non-uniform illumination image enhancement via contrast optimization and color correction," *Signal Process.*, vol. 143, pp. 210–220, Dec. 2018.
[57] Z. Al-Ameen, "Nighttime image enhancement using a new illumination boost algorithm," *IET Image Process.*, vol. 13, no. 8, pp. 1314–1320, Jun. 2019, doi: 10.1049/iet-ipr.2018.6585.
[58] A. K. Bhandari, "A logarithmic law based histogram modification scheme for naturalness image contrast enhancement," *J. Ambient Intell. Hum. Comput.*, vol. 11, no. 4, pp. 1605–1627, Apr. 2020, doi: 10.1007/s12652-019-01258-6.
[59] M. Veluchamy and B. Subramani, "Image contrast and color enhancement using adaptive gamma correction and histogram equalization," *Optik*, vol. 183, pp. 329–337, Apr. 2019, doi: 10.1016/j.ijleo.2019.02.054.

[60] Q. Zhang, G. Yuan, C. Xiao, L. Zhu, and W.-S. Zheng, "High-quality exposure correction of underexposed photos," in *Proc. ACM Multimedia Conf. Multimedia Conf. (MM)*, 2018, pp. 582–590, doi: 10.1145/3240508.3240595.
[61] J. S. Park, J. W. Soh, and N. I. Cho, "Generation of high dynamic range illumination from a single image for the enhancement of undesirably illuminated images," *Multimedia Tools Appl.*, vol. 78, no. 14, pp. 20263–20283, Jul. 2019, doi: 10.1007/s11042-019-7384-z.
[62] Z. Li, K. Cheng, and X. Wu, "Soft binary segmentation-based backlit image enhancement," in *Proc. IEEE 17th Int. Workshop Multimedia Signal Process. (MMSP)*, Oct. 2015, pp. 3–7, doi: 10.1109/MMSP.2015.7340808.
[63] U. Goel, B. Gupta, and M. Tiwari, "An efficient approach to restore naturalness of non-uniform illumination images," *Circuits, Syst., Signal Process.*, vol. 38, no. 7, pp. 3384–3398, Jul. 2019, doi: 10.1007/s00034-018-01021-w.
[64] M. Li, J. Liu, W. Yang, X. Sun, and Z. Guo, "Structure-revealing low-light image enhancement via robust retinex model," *IEEE Trans. Image Process.*, vol. 27, no. 6, pp. 2828–2841, Jun. 2018, doi: 10.1109/TIP.2018.2810539.
[65] Q. Wang, X. Fu, X.-P. Zhang, and X. Ding, "A fusion-based method for single backlit image enhancement," in *Proc. IEEE Int. Conf. Image Process. (ICIP)*, Sep. 2016, pp. 4077–4081.
[66] S.-C. Pei, C.-T. Shen, and T.-Y. Lee, "Visual enhancement using constrained l0 gradient image decomposition for low backlight displays," *IEEE Signal Process. Lett.*, vol. 19, no. 12, pp. 813–816, Dec. 2012, doi: 10.1109/LSP.2012.2220352.
[67] W. Kim, R. Lee, M. Park, and S.-H. Lee, "Low-light image enhancement based on maximal diffusion values," *IEEE Access*, vol. 7, pp. 129150–129163, 2019, doi: 10.1109/access.2019.2940452.
[68] J. Xu, Y. Hou, D. Ren, L. Liu, F. Zhu, M. Yu, H. Wang, and L. Shao, "STAR: A structure and texture aware retinex model," 2019, *arXiv:1906.06690*. [Online]. Available: http://arxiv.org/abs/1906.06690
[69] E. Reinhard, M. Stark, P. Shirley, and J. Ferwerda, "Photographic tone reproduction for digital images," in *Proc. 29th Annu. Conf. Comput. Graph. Interact. Techn. (SIGGRAPH)*, 2002, pp. 267–276.
[70] M. Yang, X. Nie, and R. W. Liu, "Coarse-to-fine luminance estimation for low-light image enhancement in maritime video surveillance," in *Proc. IEEE Intell. Transp. Syst. Conf. (ITSC)*, Oct. 2019, pp. 299–304.
[71] S. Park, S. Yu, B. Moon, S. Ko, and J. Paik, "Low-light image enhancement using variational optimization-based retinex model," *IEEE Trans. Consum. Electron.*, vol. 63, no. 2, pp. 178–184, May 2017.

ZIAUR RAHMAN received the B.S. degree in computer science from the University of Peshawar, Pakistan, in 2012, and the M.S. degree in software engineering from Chongqing University, Chongqing, China, in 2017. He is currently pursuing the Ph.D. degree with Sichuan University, Chengdu, China. His research interests include image processing, computer vision, deep learning, and fractional calculus.

PU YI-FEI received the Ph.D. degree from the College of Electronics and Information Engineering, Sichuan University, in 2006. He is currently a Full Professor and a Doctoral Supervisor with the College of Computer Science, Sichuan University, a Chief Technology Officer with Chengdu PU Chip Science and Technology Company, Ltd., and is elected into the Thousand Talents Program of Sichuan Province and the Academic and Technical Leader of Sichuan Province. He has first authored about 20 articles indexed by SCI in journals, such as *International Journal of Neural Systems*, the IEEE TRANSACTIONS ON IMAGE PROCESSING, the IEEE TRANSACTIONS ON NEURAL NETWORKS AND LEARNING SYSTEMS, the IEEE ACCESS, *Mathematical Methods in Applied Sciences, Science in China Series F: Information Sciences*, and *Science China Information Sciences*. He held several research projects, such as the National Natural Science foundation of China and the Returned Overseas Chinese Scholars Project of Education Ministry of China, and holds 13 China inventive patents, as the first or single inventor. He focuses on the application of fractional calculus and fractional partial differential equation to signal analysis, signal processing, image processing, circuits and systems, and machine intelligence.

MUHAMMAD AAMIR received the B.Eng. degree in computer systems engineering from the Mehran University of Engineering and Technology Jamshoro, Sindh, Pakistan, in 2008, the M.Eng. degree in software engineering from Chongqing University, China, in 2014, and the Ph.D. degree in computer science and technology from Sichuan University, Chengdu, China, in 2019. He is currently a Postdoctoral Fellow with the School of Communication and Information Engineering, University of Electronic Science and Technology of China, Chengdu. His main research interests include pattern recognition, computer vision, image processing, deep learning, and fractional calculus.

SAMAD WALI received the B.Sc. degree in mathematics from Forman Christian College, Lahore, Pakistan, the M.Sc. degree in applied mathematics from The Islamia University of Bahawalpur, Pakistan, and the Ph.D. degree in computational mathematics from Nankai University, Tianjin, China, in June 2018. He is currently a Postdoctoral Research Fellow in image processing and medical image analysis with the School of Communication and Information Engineering, University of Electronic Science and Technology of China, Chengdu. His main areas of research interest are image processing, variational methods, and numerical solution to partial differential equations.

YURONG GUAN graduated from the Wuhan University of Technology, in 2008. She is a Master of social computer application and an Associate Professor. She is currently working with Huanggang Normal University. Her research interests include digital image processing and Java software development.